KSÜ Tarım ve Doğa Derg 28 (2), 516-534, 2025
KSU J. Agric Nat 28 (2), 516-534, 2025
DOI:10.18016/ksutarimdoga.vi.1523681

Utilizing Plackett–Burman and Box–Behnken Designs for Plant Extract–Based AgNP Synthesis Optimization: Unveiling Antifungal Potential Against *Phytophthora* Species

Muharrem TÜRKKAN[1]
[1]Department of Plant Protection, Faculty of Agriculture, Ordu University, 52200, Ordu, Türkiye
[1]https://orcid.org/0000-0001-7779-9365
✉: muharremturkkan@odu.edu.tr

ABSTRACT

This study optimized a green synthesis method for silver nanoparticles (AgNPs) using aqueous extracts of black tea, linden, cherry laurel, kale, and melocan, employing a statistical design of experiments. The plant extracts acted as bio-reducing agents. Total and individual phenolic compounds in the extracts were quantified using ultraviolet-visible (UV–Vis) spectroscopy and ultra-high-performance liquid chromatography (UHPLC). AgNP yields were maximized through a combination of Plackett–Burman and Box–Behnken designs. The synthesized AgNPs were characterized by UV–Vis spectroscopy, Fourier transform infrared (FT–IR) spectroscopy, scanning electron microscopy (SEM) coupled with energy-dispersive X-ray spectroscopy (EDS), and transmission electron microscopy (TEM). Optimal AgNP production was achieved under the following conditions (determined by response surface methodology, RSM): 9.6 g of plant material, extraction heating at 80°C for 20 minutes, 10 mM $AgNO_3$, 2.5 mL of extract, 800 W microwave irradiation, and a 90-second reaction time. FT–IR analysis confirmed the role of phenolic compounds in reducing and stabilizing AgNPs. The resulting AgNPs exhibited uniform spherical morphology, with average particle sizes of 5.30 nm (black tea), 8.74 nm (linden), 7.20 nm (cherry laurel), 6.32 nm (kale), and 9.44 nm (melocan). Antifungal assays against five *Phytophthora* species revealed that kale-derived AgNPs were most potent, with EC_{50}, MIC, and MFC values ranging from 9.28–30.84 µg mL^{-1}, 200–300 µg mL^{-1}, and 200–400 µg mL^{-1}, respectively. These results suggest that plant-extract-synthesized AgNPs offer a sustainable approach to managing *Phytophthora* diseases, warranting further research.

Phytopathology

Research Article

Article History
Received : 28.07.2024
Accepted : 17.02.2025

Keywords
Green synthesis
Silver nanoparticle
Statistical optimization
Phytophthora spp.
Toxicity

Bitki Ekstraktı Bazlı AgNP Sentez Optimizasyonu için Plackett–Burman ve Box–Behnken Tasarımlarının Kullanımı: *Phytophthora* Türlerine Karşı Antifungal Potansiyelinin Ortaya Çıkarılması

ÖZET

Bu çalışma, siyah çay, ıhlamur, karayemiş, yaprak lahana ve melocan sulu ekstraktları kullanılarak gümüş nanoparçacıklar (AgNP'ler) için deneysel bir istatistiksel tasarım ile yeşil bir sentez yöntemini optimize etmiştir. Bu bitki ekstraktları biyo-indirgeyici ajanlar olarak işlev görmüştür. Ekstraktlardaki toplam ve bireysel fenolik bileşikler ultraviyole-görünür (UV–Vis) spektroskopi ve ultra yüksek performansli sivi kromatografisi (UHPLC) kullanılarak ölçülmüştür. AgNP verimleri, Plackett–Burman ve Box–Behnken tasarımlarının bir kombinasyonu ile maksimize edilmiştir. Sentezlenen AgNP'ler UV–Vis spektroskopisi, Fourier dönüşümlü kizilötesi (FT–IR) spektroskopisi, taramali elektron mikroskobu (SEM)-enerji dağilimli X-ışını spektroskopisi (EDS) ve geçirimli elektron mikroskopisi (TEM) ile karakterize edilmiştir. Optimum AgNP üretimi aşağıdaki koşullar altında elde edilmiştir (yanıt yüzey metodolojisi, RSM ile belirlenmiştir): 9.6 g bitki materyali, 80°C'de 20 dakika ekstraksiyon ısıtma, 10 mM $AgNO_3$, 2.5 mL ekstrakt, 800 W mikrodalga irritasyonu

Fitopatoloji

Araştırma Makalesi

Makale Tarihçesi
Geliş Tarihi : 28.07.2024
Kabul Tarihi : 17.02.2025

Anahtar Kelimeler
Yeşil sentez
Gümüş nanopartikül
Istatistiksel optimizasyon
Phytophthora spp.
Zehirlilik

ve 90 saniyelik reaksiyon süresi. FT–IR analizi, fenolik bileşiklerin AgNP indirgenmesi ve stabilize edilmesindeki rolünü göstermiştir. Elde edilen AgNP'ler 5.30 nm (siyah çay), 8.74 nm (ıhlamur), 7.20 nm (karayemiş), 6.32 nm (yaprak lahana) ve 9.44 nm (melocan) ortalama partikül boyutları ile tek tip küresel morfoloji sergilemiştir. Beş *Phytophthora* türüne karşı yapılan antifungal deneyler, yaprak lahana türevi AgNP'lerin sırasıyla 9.28-30.84 µg mL^{-1}, 200-300 µg mL^{-1} ve 200-400 µg mL^{-1} arasında değişen EC_{50}, MIC ve MFC değerleri ile en güçlü olduğunu ortaya koymuştur. Bu sonuçlar, bitki ekstraktı ile sentezlenen AgNP'lerin *Phytophthora* hastalıkların yönetiminde sürdürülebilir bir yaklaşım sunduğunu ve daha fazla araştırılması gerektiğini göstermektedir.

Atıf İçin : Türkkan, M. (2025). Bitki Ekstraktı Bazlı AgNP Sentez Optimizasyonu için Plackett–Burman ve Box–Behnken Tasarımlarının Kullanımı: Phytophthora Türlerine Karşı Antifungal Potansiyelinin Ortaya Çıkarılması. *KSÜ Tarım ve Doğa Derg 28* (2), 516-534. DOI: 10.18016/ksutarimdoga.vi.1523681.

To Cite: Türkkan, M. (2025). Utilizing Plackett–Burman and Box–Behnken Designs for Plant Extract–Based AgNP Synthesis Optimization: Unveiling Antifungal Potential Against Phytophthora Species. *KSU J. Agric Nat 28* (2), 516-534. DOI: 10.18016/ksutarimdoga.vi.1523681.

INTRODUCTION

Türkiye's Black Sea Region, with its diverse geographical and ecological conditions, harbors a rich and unique flora (Davis et al., 1988). East of the Melet River (Altınordu, Ordu), the "Colchic flora" thrives at 700–800 meters altitude along the coast—a distinct forest ecosystem dominated by moisture-loving tree and shrub species. The region's flora includes abundant forest plants, notably lime trees (*Tilia dasystyla* subsp. *caucasica* (V. Engl.) Pigott). A dense understory of small trees and shrubs further characterizes these forests (Günal, 2013). Among these, cherry laurel (*Prunus laurocerasus* L.) is valued for its fruits, ornamental qualities, and protective uses (İslam & Deligöz, 2012). Kale (*Brassica oleracea* var. *acephala* (DC.) Schltdl.), a winter dietary staple, is widely consumed in the Western and Eastern Black Sea regions (Encü, 2010), while melocan (*Smilax excelsa* L.) is integrated into spring/summer diets and folk medicine (Baytop, 1999). Tea (*Camellia sinensis* (L.) Kuntze), a culturally significant beverage, is extensively cultivated from Fatsa (Ordu) to the Türkiye-Georgia border.

These plants are rich in bioactive compounds, underpinning their pharmacological properties. Linden (*T. dasystyla* subsp. *caucasica*) contains phenols, flavonoids, aldehydes, and terpenoids (Akyüz et al., 2014; Öz, 2022). Cherry laurel (*P. laurocerasus*) is a source of protein, sugars, ascorbic acid, minerals, antioxidants, phenols, and flavonoids (Kolaylı et al., 2003; Sahan et al., 2011; Karabegović et al., 2014). Melocan (*S. excelsa*) contains phenolics, flavonoids, and anthocyanins (Özsoy et al., 2008). Kale (*B. oleracea* var. *acephala*) provides glucosinolates, polyphenols, carotenoids, minerals, vitamins, and fatty acids (Šamec et al., 2019). Black tea (*C. sinensis*) is rich in flavonoids, amino acids, vitamins, phenolic acids, lipids, proteins, volatile compounds, carbohydrates, ß-carotene, and fluoride (Naveed et al., 2018). These compounds contribute to immunomodulatory, antibacterial, antifungal, antiviral, antioxidant, and hepatoprotective effects (Yesilada et al., 1999; Kolaylı et al., 2003; Tuttu et al., 2017; Šamec et al., 2019; Naveed et al., 2018).

Growing interest in biological systems (e.g., plants, bacteria, fungi) for nanoparticle (NP) synthesis has spurred the development of green methods as sustainable alternatives to chemical approaches (Siddiqi et al., 2018). Plants, as renewable resources, offer a simple, eco-friendly route for synthesizing metallic nanoparticles (Shah et al., 2015; Siddiqi et al., 2018; Yılmaz et al., 2021). Phytochemicals in plant extracts—terpenoids, flavones, aldehydes, ketones, carboxylic acids, ascorbic acid, amides, and phenols—act as both reducing and stabilizing agents during NP synthesis (Ovais et al., 2018; Othman et al., 2019). Diverse plant parts (roots, seeds, bulbs, stems, bark, peels, petals, flowers) have been used for silver nanoparticle (AgNP) synthesis (Siddiqi et al., 2018). For example, fruit extracts of *Cnidium monnieri* (Ye et al., 2023), leaf extracts of *Phyllanthus urinaria*, *Pouzolzia zeylanica*, and *Scoparia dulcis* (Nguyen et al., 2020), and *Camellia sinensis* (white tea) (Karakaş et al., 2024), and peel extracts of *Citrus sinensis* (Miccky et al., 2023) and *C. limetta* (Trivedi et al., 2014) have demonstrated efficacy in AgNP synthesis. AgNP size and morphology can be controlled by tuning parameters like metal salt concentration, reaction time, pH, temperature, and biomaterial quantity (Sharma et al., 2022).

While traditional "one-variable-at-a-time" optimization is time-consuming, the Plackett–Burman design (PBD) offers a faster, more efficient alternative. For example, El-Sawaf et al. (2024) used PBD to identify critical factors (precursor concentrations, ratio, shaking speed, temperature, pH, incubation time) in the green synthesis of CuO/Ag/ZnO nanocomposites using *Ziziphus spina-christi* extract. Similarly, Fazil et al. (2024) optimized banana peel-AgNP synthesis via PBD, finding $AgNO_3$ concentration and incubation time as key factors. Siddiqui et al.

(2024) reported that only $AgNO_3$ concentration and incubation time significantly influenced *Salsola imbricata*-mediated AgNP synthesis. Statistical methods like PBD and response surface methodology (RSM) streamline optimization, enhancing AgNP synthesis efficiency (Halima et al., 2021; Laime-Oviedo et al., 2022). PBD identifies critical parameters, while RSM (often paired with Box–Behnken design, BBD) models optimal conditions for desired AgNP properties. This approach holds promise for agricultural and medical applications. Although PBD and RSM have been used to optimize AgNP synthesis from various plant materials, including ethanolic fractions (Laime-Oviedo et al., 2022), *Piper betle* and *Jatropha curcas* leaf extracts (Halima et al., 2021), and *Polygonum cognatum* (madimak) extracts (Türkkan & Gürel, 2024), their application to black tea, linden, cherry laurel, kale, and melocan remains unexplored, a gap addressed by this study.

The present study optimized AgNP synthesis from five plant extracts using PBD and BBD. The AgNPs were characterized via UV–Vis spectroscopy, FT–IR, SEM–EDS, and TEM to assess physicochemical properties. Their antifungal potential was evaluated against multiple *Phytophthora* species.

MATERIAL and METHOD

Plant Collection and Preparation

Plant specimens were collected from their natural habitats during the growing season. Specifically, kale (*Brassica oleracea* var. *acephala* – leaves), linden (*Tilia dasystyla* subsp. *caucasica* – flowers and leaves), and cherry laurel (*Prunus laurocerasus* – leaves) were obtained from Gülyalı, Ordu; black tea (*Camellia sinensis* – leaves) from Fındıklı, Rize; and melocan (*Smilax excelsa* – shoots and leaves) from Çarşamba, Samsun.

Chemicals and Reagents

Silver nitrate ($AgNO_3$), sodium hydroxide (NaOH), gallic acid (GA), Folin-Ciocalteu reagent, sodium bicarbonate, and all other chemicals were purchased from Sigma-Aldrich (Sigma Aldrich Chemie GmbH, Steinheim, Germany).

Phytophthora Isolates

The *Phytophthora* isolates used in this study were obtained from the Batı Akdeniz Agricultural Research Institute (BATEM) and maintained in the mycology culture collection of the Department of Plant Protection, Faculty of Agriculture at Ordu University.

Preparation of Aqueous Extracts from Plants

Freshly collected plant specimens were washed with tap water to remove initial impurities and then rinsed three times with distilled water. The cleaned plants were cut into smaller pieces and dried at 60°C for 3–4 days to facilitate efficient extraction of bioactive compounds. To optimize the extraction process for silver nanoparticle (AgNP) synthesis, we investigated the influence of plant material amount (5, 7.5, or 10 g), extraction heating time (20 or 30 minutes), and extraction heating temperature (60, 70, or 80°C). For extraction, weighed portions of chopped plant material were added to individual 250 mL beakers containing 100 mL of distilled water and heated at the predetermined temperature for the indicated time. After cooling to room temperature, the extracts were filtered through Whatman No. 1 filter paper and centrifuged at 10,000 rpm for 10 minutes to remove any remaining plant material. The resulting extracts were stored at 4°C until used as reducing and stabilizing agents in AgNP synthesis.

Phenolic Profile of Plant Extracts: Total Content and Individual Compounds

The total phenolic content of the plant extracts was determined using the Folin-Ciocalteu assay (Singleton & Rossi, 1965). Briefly, 600 µL of extract was diluted with 4 mL distilled water and mixed with 600 µL of 10% Folin-Ciocalteu reagent. After a 5-minute dark incubation, 300 µL of 2% sodium bicarbonate was added, and the mixture was allowed to stand for 2 hours. Absorbance was then measured at 760 nm using a UV–Vis spectrophotometer (Lambda 35, Perkin Elmer Inc., Hopkinton, MA, USA). Gallic acid (5–100 µg mL^{-1}) served as the standard for quantification, with results expressed as gallic acid equivalents (GAE) g kg^{-1}. Individual phenolic compounds were identified and quantified using ultra-high-performance liquid chromatography (UHPLC, Thermo Fisher Scientific Inc., Ultimate-3000, Waltham, MA, USA) coupled with a diode array detector (DAD 3000, Thermo Fisher Scientific Inc.), following a modified protocol from Ozturk et al. (2015). Dried plant material was suspended in methanol and centrifuged to remove debris. The supernatant was filtered and injected into the UHPLC system. Separation was achieved on a Hypersil GD column (Thermo Fisher Scientific Inc., USA) using a gradient of aqueous formic acid and methanol. Detection was set at 274 nm, with a 60-minute run time, 20 µL injection volume, and a 1.0 mL min^{-1}

flow rate. Concentrations were determined from peak areas compared to a standard curve of known phenolic standards and expressed as mg kg^{-1} of dry plant material.

Synthesis of Silver Nanoparticles (AgNPs)

Plant extract (2.5–7.5 mL) was added dropwise to 25 mL of silver nitrate ($AgNO_3$) solution (1–10 mM). The mixture's pH was adjusted to 10 using 0.1 M sodium hydroxide (NaOH). Microwave irradiation (600–800 W, 30–90 seconds) reduced the silver ions (Ag^+) to metallic silver nanoparticles (AgNPs), indicated by a color change from light yellow to brown or dark brown. AgNP formation was confirmed by UV–Vis spectroscopy (200–700 nm). AgNP yield, corresponding to 5–50 nm sized particles (Noroozi et al., 2012; Chowdhury et al., 2016), was estimated from the area under the spectral curve (350–420 nm) using the following equation (Eq. 1):

$$Y = \sum (a_i + a_{i+1})/2 \; x \; (w_{i+1} - w_i)$$

where Y is the response (area), a is the absorbance, and w is the wavelength.

Optimization of Synthesized AgNP

To maximize AgNP yield and optimize the synthesis process, Plackett–Burman design (PBD) and the Box–Behnken design (BBD) were employed.

Plackett–Burman Design (PBD): Unveiling Key Factors

A Plackett–Burman design (PBD) was used to screen the most influential factors affecting plant-mediated AgNP synthesis. Seven variables were investigated: plant material quantity (g), extraction heating temperature (°C), extraction heating time (min), $AgNO_3$ concentration (mM), extract volume (mL), microwave power (W), and reaction time (sec). Each factor (A-G) was tested at two levels (+1 and −1), with upper and lower limits selected based on preliminary experiments. A 12-run PBD matrix was generated in Microsoft Excel, encompassing all high/low combinations (Table 1). AgNP yield, indirectly measured by UV–Vis spectroscopy (spectral area 350–420 nm), served as the response variable. The spectral area data were then analyzed using Minitab software (version 19.2; Minitab, Inc., USA).

PBD is based on the first-order linear model equation (Eq. 2) (Plackett & Burman, 1946):

$$Y = \beta_0 + \sum \beta_i x_i$$

where Y is the response (area), ß0 is the model intercept, Xi is the level of each independent variable, and ßi is the linear coefficient.

Table 1. Experimental factors and responses in Plackett–Burman design for AgNP synthesis
Çizelge 1. AgNP sentezi için Plackett–Burman tasarımındaki deneysel faktörler ve yanıtlar

Run	Independent variables							Response: Area (350–420 nm)				
	A[a]	B[b]	C[c]	D[d]	E[e]	F[f]	G[g]	Black tea	Linden	Cherry laurel	Kale	Melocan
1	10	60	20	1	7.5	400	30	-1.42	1.05	5.18	1.44	10.45
2	5	80	30	1	2.5	800	30	-1.95	2.36	3.88	-0.64	-2.29
3	5	60	30	10	2.5	400	90	28.50	17.79	26.49	13.92	27.71
4	10	60	20	1	7.5	400	30	1.12	1.54	5.05	2.06	10.34
5	5	80	20	10	2.5	800	30	24.87	16.55	27.17	11.19	21.80
6	5	60	30	1	2.5	400	90	-0.15	2.47	2.95	-1.38	0.69
7	10	60	30	10	2.5	400	30	22.21	15.53	23.55	16.71	22.53
8	5	80	20	10	7.5	400	30	18.83	18.38	22.74	13.10	16.86
9	10	60	30	1	7.5	800	90	4.97	4.49	15.18	10.10	26.99
10	10	80	20	10	2.5	800	90	59.07	52.95	56.07	43.04	55.16
11	5	80	20	1	7.5	800	90	0.62	3.76	7.74	5.83	7.77
12	10	80	30	10	7.5	800	90	50.36	45.88	43.71	32.38	35.98

[a]Amount of plant material (g) (A), [b]Extraction heating temperature (°C) (B), [c]Extraction heating time (min.) (C), [d]Concentration of $AgNO_3$ (mM) (D), [e]Extract volume (mL) (E), [f]Power of microwave (W) (F), [g]Reaction time (s) (G)

Regression analysis and ANOVA (analysis of variance) were employed to evaluate the significance of each factor's effect on the response variable. Statistical analysis revealed factors significantly affecting the yield of synthesized AgNPs.

Box–Behnken Design (BBD): Optimizing Key Factors

Following the Plackett–Burman design (PBD) analysis, a Box–Behnken design (BBD) was implemented to optimize the most influential factors affecting AgNP yield. This involved a 15-run experimental design, where each factor was tested at three levels: low (−1), medium (0), and high (+1) (Table 2). This allowed for a comprehensive analysis of the relationships between factors and AgNP yield, quantified as the spectral area (λ = 350–420 nm) using UV–Vis spectroscopy.

Minitab software (version 19.2; Minitab, Inc., USA) was used for experimental design, regression analysis, and graphical data representation. The response variable was fitted to a second-order polynomial model (Eq. 3) (Box & Behnken, 1960):

$$Y = \beta_0 + \sum_i \beta_i X_i + \sum_{ii} \beta_{ii} X_i^2 + \sum_{ij} \beta_{ij} X_i X_j$$

where Y is the response, Xi is the coded level of the independent variable, ß0 is the regression coefficient, ßi is the linear coefficient, ßii is the quadratic coefficient, and ßij is the interaction coefficient.

Statistical analysis of the BBD data revealed interactions between factors and their combined effects on AgNP yield. The quadratic and interaction terms provided critical insights into these complex relationships.

Table 2. Experimental factors and responses in Box–Behnken design for AgNP synthesis
Çizelge 2. AgNP sentezi için Box–Behnken tasarımındaki deneysel faktörler ve yanıtlar

Std[a]	Run	Independent variables			Response: Area (350–420 nm)				
		A[b]	D[c]	G[d]	Black tea	Linden	Cherry laurel	Kale	Melocan
5	1	5	5.5	30	15.11	16.43	18.64	12.59	18.73
7	2	5	5.5	90	27.45	29.32	33.80	25.07	31.80
3	3	5	10	60	40.82	26.56	36.67	25.46	38.62
9	4	7.5	1	30	4.56	3.83	3.73	2.59	3.25
15	5	7.5	5.5	60	20.02	20.12	23.34	17.22	22.63
13	6	7.5	5.5	60	21.43	20.79	22.59	18.05	24.40
14	7	7.5	5.5	60	20.57	21.02	22.46	17.30	23.29
1	8	5	1	60	2.72	2.96	3.55	2.94	4.67
6	9	10	5.5	30	17.12	17.086	19.06	12.65	18.08
8	10	10	5.5	90	35.27	31.77	36.09	25.85	39.37
2	11	10	1	60	3.44	3.11	4.98	3.35	5.83
12	12	7.5	10	90	58.47	46.45	57.75	45.06	54.52
11	13	7.5	1	90	4.92	5.82	6.06	5.60	7.54
10	14	7.5	10	30	27.73	19.20	29.03	19.88	29.50
4	15	10	10	60	43.38	32.78	39.14	28.61	42.61

[a]Std is the standard order, [b]Amount of plant material (g) (A), [c]Concentration of $AgNO_3$ (mM) (D), [d]Reaction time (s) (G)

Characterization of Synthesized AgNPs

Synthesized AgNPs were characterized using several techniques. Ultraviolet–Vis (UV–Vis) spectroscopy was performed by diluting 20 µl of AgNP solution with 2 mL of distilled water and analyzing the sample at a 1 nm resolution between 200 and 700 nm using a quartz cuvette and a distilled water blank for baseline correction. For Fourier Transform Infrared (FT–IR) spectroscopy (Spectrum 65, Perkin Elmer Inc., Hopkinton, MA, USA), 1 mg of AgNPs was mixed with 200 mg of potassium bromide (KBr), pressed into a pellet, and scanned in transmittance mode from 4000 to 400 cm^{-1}. Elemental analysis was performed using scanning electron microscopy (SEM) coupled with energy-dispersive X-ray spectroscopy (EDS) (SU-1510, Hitachi High-Tech., Tokyo, Japan). Particle size and structure were confirmed by transmission electron microscopy (TEM) (HT7700, Hitachi High-Tech., Tokyo, Japan). Particle size distribution, determined from TEM images using ImageJ (National Institutes of Health, USA), was fitted to a Gaussian function using OriginPro software (2019b version 9.6.5.169, OriginLab Corporation, USA).

Antifungal Efficacy of Synthesized AgNPs Against *Phytophthora* Species

The antifungal efficacy of synthesized AgNPs against *P. capsici*, *P. cinnamomi*, *P. citrophthora*, *P. nicotianae*, and *P. palmivora* was determined following the method described by Gevrek et al. (2023). AgNPs were added to sterilized V8 agar media at concentrations of 50, 100, 200, 300, and 400 µg mL^{-1} and cooled to 50°C. The modified medium was dispensed into Petri dishes, with unmodified V8 agar serving as a control. Mycelial discs (5 mm diameter) from 7-day-old fungal cultures were inoculated at the center of each Petri dish. Plates were incubated in darkness at 25°C until control plates were fully colonized (4–7 days). Fungal colony diameters were measured

perpendicularly to assess growth inhibition. The percentage of mycelial growth inhibition (MGI) was calculated using the formula: MGI (%) = [(dc − dt) / dc] × 100, where dc represents the colony diameter on control plates and dt represents the colony diameter on treated plates (measured in two perpendicular directions).

The fungicidal efficacy of the synthesized AgNPs was evaluated using EC_{50} values (the concentration inhibiting 50% of fungal growth), determined by probit analysis in SPSS (v. 22, IBM, Chicago, USA). The minimum inhibitory concentration (MIC), defined as the lowest concentration completely preventing fungal growth, was also determined. To confirm fungicidal activity and establish the minimum fungicidal concentration (MFC), agar disks from treated plates exhibiting no visible growth were subcultured onto fresh V8 agar and incubated at 25°C for 9 days.

RESULTS and DISCUSSION

Exploring the Bioactive Profile of Plant Extracts and Their Role in AgNP Synthesis

This study employed a biocompatible approach to synthesize highly efficient, spherical AgNPs using aqueous extracts of black tea, linden, cherry laurel, kale, and melocan as reducing and stabilizing agents. Total phenolic content, measured via the Folin-Ciocalteu (F-C) method (Singleton et al., 1999), varied across the extracts: black tea (4.07 g kg^{-1} GAE), linden (4.87 g kg^{-1} GAE), cherry laurel (6.66 g kg^{-1} GAE), melocan (1.81 g kg^{-1} GAE), and kale (5.56 g kg^{-1} GAE). UHPLC analysis revealed diverse phenolic profiles for each extract (Table 3). Identified phenolic compounds, including aminobenzoic acid, protocatechuic acid, hydroxybenzoic acid, caffeic acid, coumaric acid, ferulic acid, and rutin, likely played a crucial role in the bioreduction of silver ions (Ag^+) to AgNPs. These findings align with previous studies highlighting plant-derived phenolics as key agents in AgNP synthesis. For example, Kumar et al. (2012) attributed Ag^+ reduction in *Terminalia chebula* extract to its polyphenol content, suggesting these compounds act as both reducing and stabilizing agents. Similarly, Ahmed and Sharma (2012) reported that phenolics in pineapple (*Ananas comosus*) exhibit strong antioxidant activity due to their free radical scavenging capacity. Firoozi et al. (2016) further demonstrated that phenolics in *Satureja intermedia* extract (leaves, stems, and flowers) facilitate Ag^+ reduction to nanoparticles.

During microwave-assisted AgNP synthesis, the addition of plant extracts to aqueous $AgNO_3$ solution resulted in a color change from light yellow to dark brown, indicating AgNP formation via surface plasmon resonance (SPR). As shown in Figure 1(a–b), the AgNPs exhibited a prominent surface plasmon resonance (SPR) peak between 402 and 409 nm, consistent with the observed dark brown coloration. The sharp SPR peak confirmed Ag^+ reduction and suggested high monodispersity (Konwarh et al., 2011). While SPR peak characteristics are influenced by factors beyond size distribution—such as shape, morphology, composition, and the surrounding dielectric environment (Kelly et al., 2003; Stepanov, 2004)—the observed narrow peak width implies a relatively uniform AgNP size distribution.

Table 3. Phenolic acid content in plant extracts
Çizelge 3. Bitki ekstraktlarındaki fenolik asit içeriği

Phenolic compounds	Black tea	Linden	Cherry laurel	Kale	Melocan
			(mg kg^{-1} fw)		
4-Aminobenzoic acid	292.68	46.38	0.94	2.25	0.64
Protocatechuic acid	0.24	77.90	0.54	9.41	0.45
4-Hydroxybenzoic acid	4.21	-	-	2215.3	0.37
Catechin	-	5.76	3.40	10.07	0.26
Chlorogenic acid	-	-	0.73	-	-
Caffeic acid	6.54	24.83	10.92	4.88	7.79
Epicatechin	7.07	7.27	1.62	0.83	-
p-Coumaric acid	30.78	10.26	0.78	5.03	3.55
Ferulic acid	3.82	52.80	5.18	7.20	-
Rutin	42.99	0.18	18.07	1.86	11.85

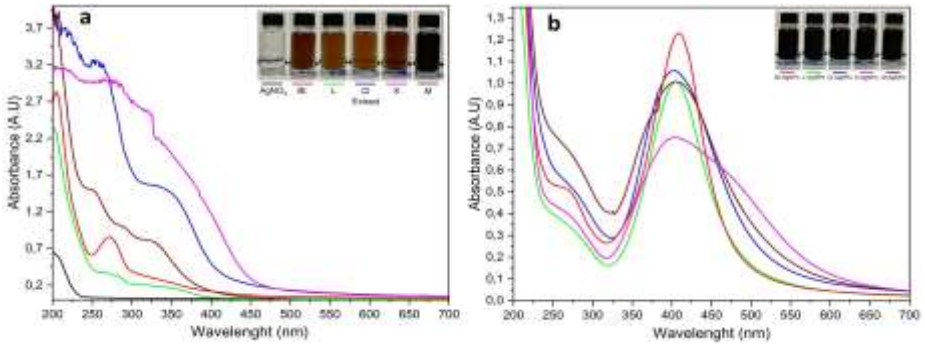

Figure 1. UV–Vis absorption spectra of (a) aqueous extracts of black tea (Bt), linden (L), cherry laurel (Cl), kale (K), and melocan (M), and (b) their corresponding synthesized AgNPs (Bt-AgNPs, L-AgNPs, Cl-AgNPs, K-AgNPs, M-AgNPs) under optimized conditions.

Şekil 1. Siyah çay (Bt), ıhlamur (L), karayemiş (Kl), yaprak lahana (K) ve melocan (M) sulu ekstraktlarının (a) ve bunlara karşılık gelen sentezlenmiş AgNP'lerin (BT-, L-, KL-, K- ve M-AgNP'ler) optimize edilmiş koşullar altında (b) UV–Vis absorpsiyon spektrumları.

Statistical Optimization of The Synthesized AgNPs

Plackett–Burman design (PBD)

Table 1 presents the Plackett–Burman design (PBD) matrix and corresponding AgNP yields for each experimental run. The observed yields varied widely across plant species: black tea (−1.95 to 59.07), linden (1.05 to 52.95), cherry laurel (5.05 to 56.07), kale (−1.38 to 43.04), and melocan (−2.29 to 55.16), underscoring the need for optimization. Figure 2(a–e) shows the UV–Vis spectra from these runs.

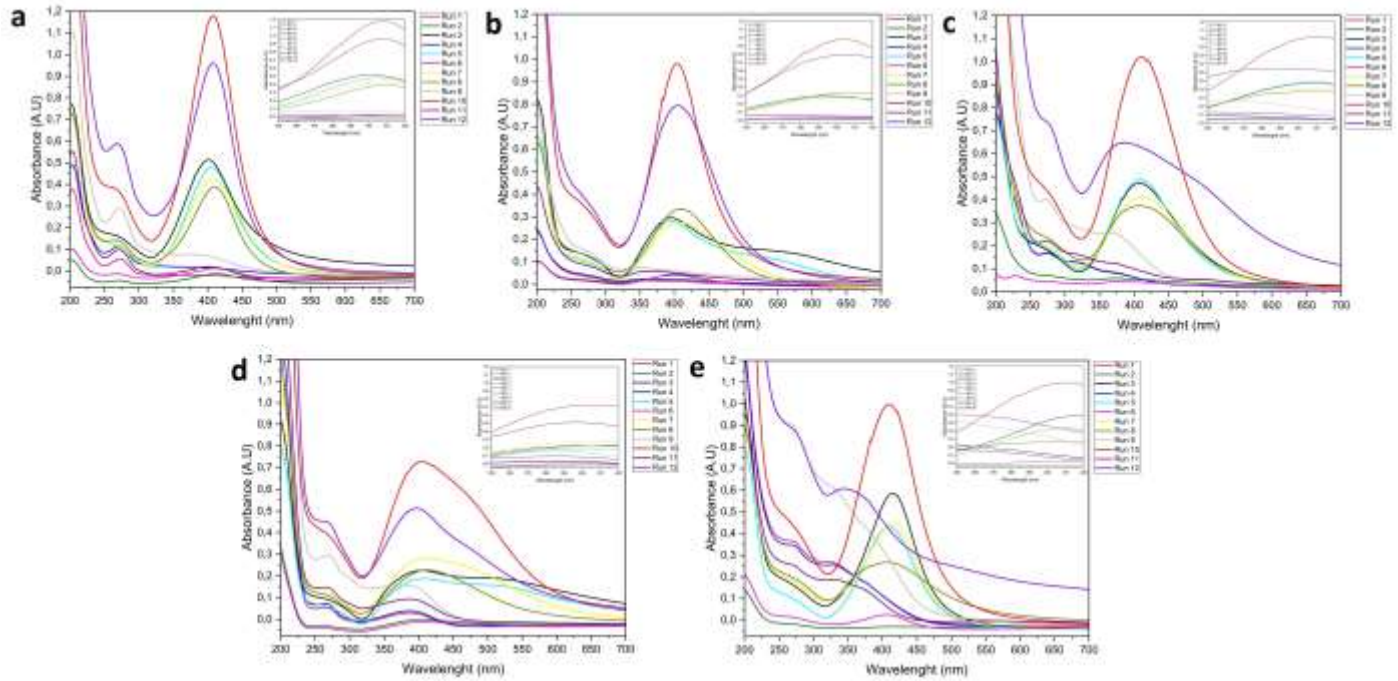

Figure 2. UV–Vis absorption spectra of silver nanoparticles synthesized using Plackett–Burman design parameters: Bt-AgNPs (a), L-AgNPs (b), Cl-AgNPs (c), K-AgNPs (d), and M-AgNPs (e).

Şekil 2. Plackett–Burman deney tasarımı parametreleri kullanılarak sentezlenmiş gümüş nanopartiküllerin UV–Vis absorpsiyon spektrumları: Bt-AgNP'ler (a), L-AgNP'ler (b), Cl-AgNP'ler (c), K-AgNP'ler (d) ve M-AgNP'ler (e).

Statistical analysis of the PBD data confirmed the model's significance (F- and p-values), indicating a strong relationship between the investigated factors and AgNP yield (Table 4). Plant material quantity (A), $AgNO_3$ concentration (D), and reaction time (G) significantly and positively influenced AgNP yield ($p < 0.05$), with standardized effects ranging from 14.23–21.22, 12.72–25.05, and 11.78–15.70, respectively. Extraction heating temperature (B) also positively impacted yield, albeit with lower confidence (except for melocan, which exhibited

a negative effect). Conversely, extraction heating time (C), extract volume (E), and microwave power (F) adversely affected yield. These results highlight the critical role of plant species in determining key factors for AgNP biosynthesis. Previous studies report similar variations in influential parameters depending on plant material. For example, Trivedi et al. (2014) identified temperature, illumination, and pH as critical parameters for AgNP synthesis from citrus peel extract using PBD. Halima et al. (2021) found plant extract and $AgNO_3$ concentration to be most influential in PBD optimization of *Piper betle* and *Jatropha curcas* leaf extract-mediated AgNP synthesis. More recently, Fazil et al. (2024) utilized PBD to optimize banana peel-AgNP synthesis, determining that only $AgNO_3$ concentration and incubation time were statistically significant among the four factors investigated ($AgNO_3$ concentration, incubation temperature, incubation time, and plant/$AgNO_3$ ratio).

Table 4. Statistical analysis of Plackett–Burman design for AgNP yield optimization
Çizelge 4. AgNP verim optimizasyonu için Plackett–Burman tasarımının istatistiksel analizi

Variables	Effect	Coefficient	*t*-value	*F*-value	*p*-value	Confidense (%)
Black tea						
Model		17.253		24.464	0.0039	99.99
A:Amount of plant material (g)	19.32	9.659	4.488	20.141	0.011	98.91
B:Extraction heating temperature (°C)	16.59	8.294	2.348	5.513	0.079	92.13
C:Extraction heating time (min.)	-2.42	-1.210	-0.633	0.401	0.561	43.90
D:Concentration of $AgNO_3$ (mM)	25.05	12.527	5.820	33.878	0.004	99.57
E:Extract volume (mL)	-8.57	-4.285	-2.154	4.642	0.097	90.25
F:Power of microwave (W)	-4.82	-2.409	-0.797	0.636	0.470	53.01
G:Reaction time (s)	15.70	7.849	4.290	18.402	0.013	98.73
Linden						
Model		15.230		23.650	0.0042	99.99
A:Amount of plant material (g)	21.22	10.609	5.786	33.483	0.004	99.56
B:Extraction heating temperature (°C)	25.69	12.843	4.268	18.219	0.013	98.70
C:Extraction heating time (min.)	-0.25	-0.124	-0.076	0.006	0.943	5.70
D:Concentration of $AgNO_3$ (mM)	14.04	7.020	3.829	14.661	0.019	98.14
E:Extract volume (mL)	-7.90	-3.950	-2.331	5.435	0.080	91.99
F:Power of microwave (W)	-10.81	-5.406	-2.100	4.411	0.104	89.64
G:Reaction time (s)	15.68	7.839	5.029	25.294	0.007	99.27
Cherry laurel						
Model		19.977		31.805	0.0024	99.99
A:Amount of plant material (g)	14.78	7.388	4.805	23.093	0.009	99.14
B:Extraction heating temperature (°C)	9.57	4.784	1.896	3.595	0.131	86.92
C:Extraction heating time (min.)	-4.06	-2.031	-1.488	2.213	0.211	78.89
D:Concentration of $AgNO_3$ (mM)	21.48	10.739	6.984	48.782	0.002	99.78
E:Extract volume (mL)	-5.87	-2.937	-2.067	4.273	0.108	89.24
F:Power of microwave (W)	0.99	0.496	0.230	0.053	0.830	17.04
G:Reaction time (s)	11.78	5.892	4.508	20.323	0.011	98.92
Kale						
Model		12.312		48.477	0.0010	99.99
A:Amount of plant material (g)	16.72	8.361	8.400	70.552	0.001	99.89
B:Extraction heating temperature (°C)	13.27	6.634	4.061	16.492	0.015	98.47
C:Extraction heating time (min.)	-2.14	-1.070	-1.211	1.466	0.293	70.73
D:Concentration of $AgNO_3$ (mM)	12.72	6.361	6.390	40.829	0.003	99.69
E:Extract volume (mL)	-5.04	-2.518	-2.737	7.493	0.052	94.80
F:Power of microwave (W)	-3.46	-1.730	-1.238	1.532	0.284	71.65
G:Reaction time (s)	11.87	5.936	7.015	49.206	0.002	99.78
Melocan						
Model		19.500		11.730	0.0157	99.98
A:Amount of plant material (g)	14.23	7.116	3.012	9.075	0.039	96.05
B:Extraction heating temperature (°C)	-5.08	-2.542	-0.656	0.430	0.548	45.22
C:Extraction heating time (min.)	-8.75	-4.375	-2.086	4.351	0.105	89.47
D:Concentration of $AgNO_3$ (mM)	21.60	10.799	4.572	20.899	0.010	98.98
E:Extract volume (mL)	-3.33	-1.665	-0.763	0.581	0.488	51.18
F:Power of microwave (W)	8.71	4.357	1.314	1.726	0.259	74.08
G:Reaction time (s)	12.45	6.223	3.099	9.605	0.036	96.38

Optimization of AgNP synthesis parameters using Box–Behnken design (BBD)

Based on the PBD results, a three-level Box–Behnken design (BBD) was used to optimize the three most significant factors: plant material quantity (A), $AgNO_3$ concentration (D), and reaction time (G). Fifteen experiments were conducted, and the resulting AgNP yields and UV–Vis spectra are presented in Table 2 and Figure 3(a–e). Response surface methodology (RSM) analysis showed a strong, highly significant model ($p < 0.0001$) for silver nanoparticle (AgNP) yield from black tea, linden, cherry laurel, kale, and melocan (Table 5). High F-values (314.43, 400.51, 148.42, 86.24, and 305.66, respectively) confirmed these strong effects. Plant material quantity (A), silver nitrate concentration (D), and reaction time (G) significantly influenced AgNP yield ($p < 0.05$, $p < 0.0001$, and $p < 0.0001$, respectively), except for plant material quantity in cherry laurel and kale. The interaction between silver nitrate concentration and reaction time (DG) was also significant ($p < 0.001$). While the quadratic term for plant quantity (A^2) was non-significant, the quadratic terms for silver nitrate concentration (D^2) and reaction time (G^2) were generally significant ($p < 0.05$). High R^2 values (0.99812, 0.9986, 0.9963, 0.9936, and 0.9982, respectively) demonstrated the model's excellent predictive power, approaching the ideal value of 1. Non-significant lack-of-fit F-values (3.72, 4.00, 17.99, 18.50, and 1.81, respectively) further confirmed the model's suitability. A second-order regression model was developed to predict AgNP yield based on these factors (Table 5).

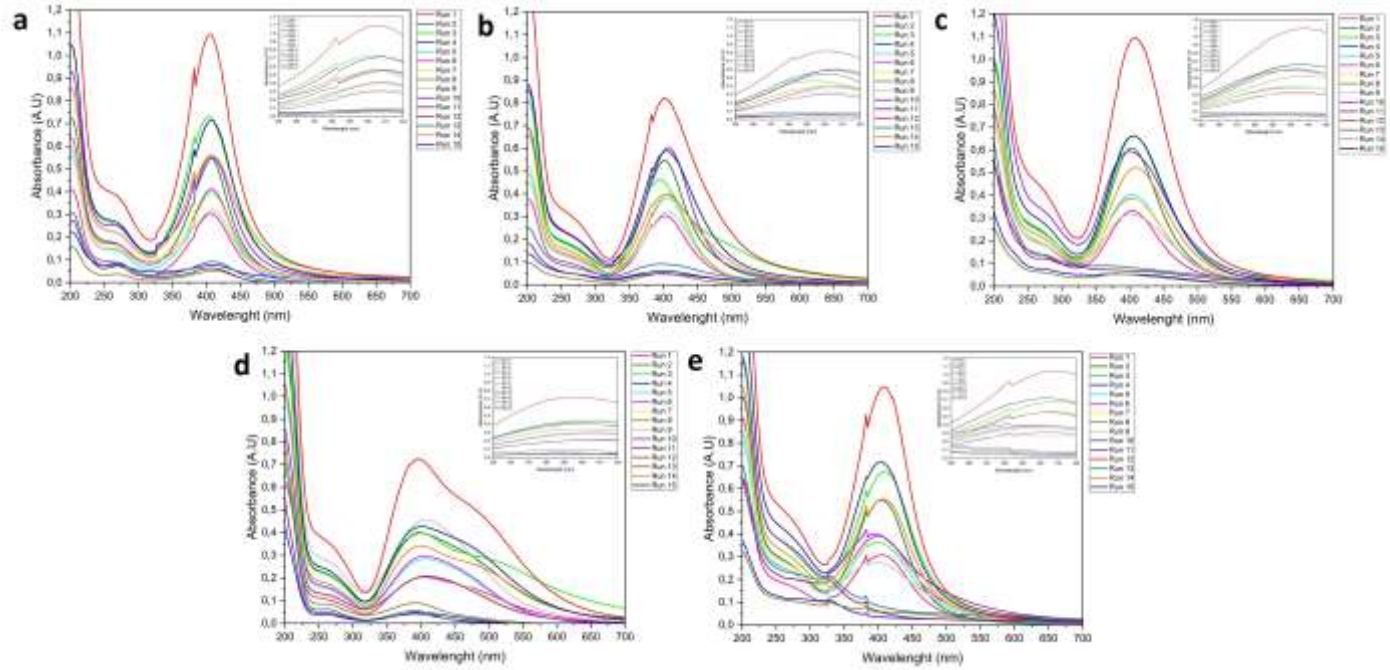

Figure 3. UV–Vis absorption spectra of silver nanoparticles synthesized using Box–Behnken design parameters: Bt-AgNPs (a), L-AgNPs (b), Cl-AgNPs (c), K-AgNPs (d), and M-AgNPs (e).

Şekil 3. Box–Behnken deney tasarımı parametreleri kullanılarak sentezlenmiş gümüş nanopartiküllerin UV–Vis absorpsiyon spektrumları: Bt-AgNP'ler (a), L-AgNP'ler (b), Cl-AgNP'ler (c), K-AgNP'ler (d) ve M-AgNP'ler (e).

The 3D and 2D response surface plots illustrate the key interactions influencing AgNP yield (Figure 4a–g). These visualizations depict the combined effects of plant material quantity, silver nitrate concentration, and reaction time. In general, maximizing silver nitrate concentration and reaction time, while maintaining plant material quantity at 7.5 g, resulted in higher AgNP yields (Figure 4a–c, 4e, and 4g). Further analysis suggests that plant material quantity had minimal impact on yield (Figure 4d and 4f). However, a synergistic interaction between silver nitrate concentration and reaction time was evident, with the highest yield achieved when both factors were at their maximum levels. These findings align with previous studies on AgNP synthesis using linden flower, hazelnut leaf, and madimak plant extracts (Gevrek et al., 2023; Yiğit & Türkkan, 2023; Türkkan & Gürel, 2024). Our results also reinforce the significance of optimizing "total energy" (power × time) for high-quality AgNP synthesis. This is consistent with the observations of Cai et al. (2017), who reported that insufficient total energy (<700 W min 100 mL^{-1}) limited complete silver ion reduction. Similarly, Nikaeen et al. (2020) observed a positive correlation between both silver nitrate concentration and reaction time with AgNP quality.

Table 5. Statistical analysis of Box–Behnken design for AgNP yield optimization
Çizelge 5. AgNP verim optimizasyonu için Box–Behnken tasarımının istatistiksel analizi

Source	Sum of squares	DF	Mean square	*F*-value	*p*-value	R^2	Adj. R^2	Pred R^2
Black tea								
Model	3751.36	9	416.82	314.43	0.000	0.9982	0.9951	0.9755
A:Amount of plant material (g)	21.53	1	21.53	16.24	0.01			
D:Concentration of $AgNO_3$ (mM)	2993.65	1	2993.7	2258.32	< 0.0001			
G:Reaction time (s)	474.12	1	474.12	357.66	< 0.0001			
AD	0.8445	1	0.8445	0.637	0.461			
AG	8.44	1	8.44	6.37	0.053			
DG	230.59	1	230.59	173.95	< 0.0001			
A^2	2.77	1	2.77	2.09	0.2083			
D^2	4.07	1	4.07	3.07	0.1402			
G^2	17.8	1	17.8	13.42	0.0145			
Residual	6.63	5	1.33					
Lack of fit	5.62	3	1.87	3.72	0.219			
Pure error	1.01	2	0.50					
Corrected total	3757.99	14						
$Y=20.67+1.64A+19.34D+7.70G+0.46AD+1.45AG+7.59DG+0.87A^2+1.05D^2+2.20G^2$								
Linden								
Model	2189.60	9	243.29	400.51	0.000	0.9986	0.9961	0.9806
A:Amount of plant material (g)	11.2	1	11.2	18.44	0.0078			
D:Concentration of $AgNO_3$ (mM)	1492.22	1	1492.2	2456.55	< 0.0001			
G:Reaction time (s)	403.75	1	403.75	664.66	< 0.0001			
AD	9.2	1	9.2	15.14	0.0115			
AG	0.8118	1	0.8118	1.34	0.2999			
DG	159.54	1	159.54	262.64	< 0.0001			
A^2	0.2619	1	0.2619	0.4312	0.5404			
D^2	76.77	1	76.77	126.39	< 0.0001			
G^2	27.75	1	27.75	45.68	0.0011			
Residual	3.04	5	0.61					
Lack of fit	2.60	3	0.87	4.00	0.206			
Pure error	0.43	2	0.22					
Corrected total	2192.63	14						
$Y=20.64+1.18A+13.66D+7.10G+1.52AD+0.45AG+6.32DG+0.27A^2-4.56D^2+2.74G^2$								
Cherry laurel								
Model	3353.69	9	372.63	148.42	0.000	0.9963	0.9896	0.9422
A:Amount of plant material (g)	5.47	1	5.47	2.18	0.1998			
D:Concentration of $AgNO_3$ (mM)	2601.68	1	2601.7	1036.29	< 0.0001			
G:Reaction time (s)	500.08	1	500.08	199.19	< 0.0001			
AD	0.2732	1	0.2732	0.1088	0.7548			
AG	0.871	1	0.871	0.347	0.5814			
DG	174.05	1	174.05	69.33	0.0004			
A^2	1	1	1	0.4003	0.5548			
D^2	18.42	1	18.42	7.34	0.0423			
G^2	47.22	1	47.22	18.81	0.0075			
Residual	12.55	5	2.51					
Lack of fit	12.10	3	4.03	17.99	0.053			
Pure error	0.45	2	0.22					
Corrected total	3366.25	14						
$Y=22.80+0.83A+18.03D+7.91G+0.26AD+0.47AG+6.60DG+0.52A^2-2.23D^2+3.58G^2$								
Kale								
Model	1891.39	9	210.15	86.24	0.000	0.9936	0.9821	0.9007
A:Amount of plant material (g)	2.41	1	2.41	0.9901	0.3654			
D:Concentration of $AgNO_3$ (mM)	1366.09	1	1366.1	560.62	< 0.0001			
G:Reaction time (s)	362.75	1	362.75	148.86	< 0.0001			
AD	1.88	1	1.88	0.7723	0.4197			
AG	0.132	1	0.132	0.0541	0.8252			
DG	122.97	1	122.97	50.46	0.0009			
A^2	2.6	1	2.6	1.07	0.3489			
D^2	9.38	1	9.38	3.85	0.1071			
G^2	20.48	1	20.48	8.4	0.0338			

Residual	12.18	5	2.44					
Lack of fit	11.76	3	3.92	18.50	0.052			
Pure error	0.42	2	0.21					
Corrected total	1903.57	14						
$Y=17.52+0.55A+13.07D+6.73G+0.69AD+0.18AG+5.54DG-0.84A^2-1.59D^2+2.35G^2$								
Melocan								
Model	3282.11	9	364.68	305.66	0.000	0.9982	0.9949	0.9777
A:Amount of plant material (g)	18.2	1	18.2	15.26	0.0113			
D:Concentration of $AgNO_3$ (mM)	2590.59	1	2590.6	2171.35	< 0.0001			
G:Reaction time (s)	506.74	1	506.74	424.73	< 0.0001			
AD	2	1	2	1.68	0.2516			
AG	16.89	1	16.89	14.16	0.0131			
DG	107.54	1	107.54	90.14	0.0002			
A^2	7.17	1	7.17	6.01	0.0578			
D^2	13.3	1	13.3	11.14	0.0206			
G^2	17.26	1	17.26	14.47	0.0126			
Residual	5.97	5	1.19					
Lack of fit	4.36	3	1.45	1.81	0.375			
Pure error	1.61	2	0.80					
Corrected total	3288.08	14						
$Y=23.44+1.51A+18.00D+7.96G+0.71AD+2.05AG+5.19DG+1.39A^2-1.90D^2+2.16G^2$								

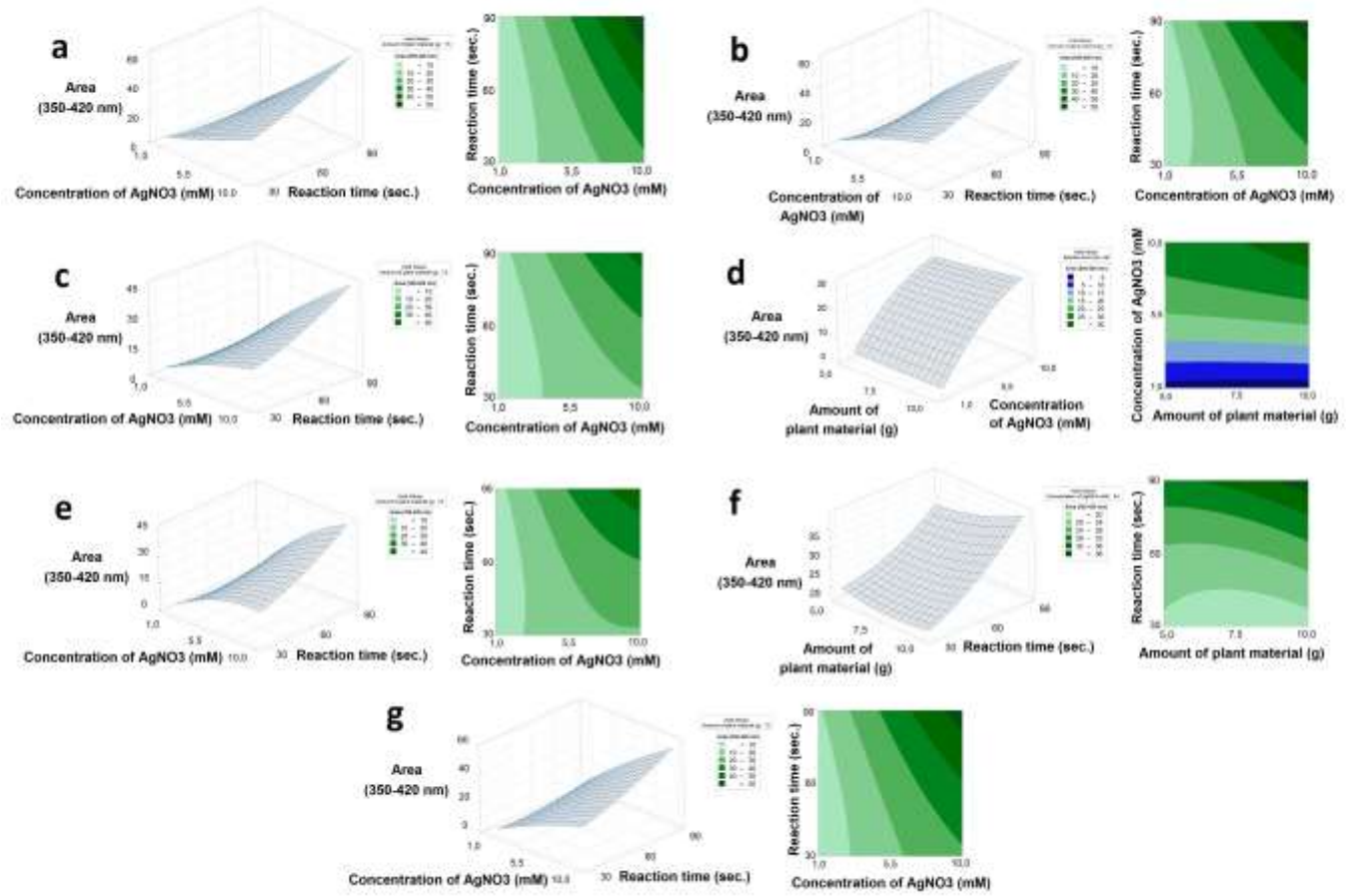

Figure 4. Influence of process parameters on AgNP yield (as determined by UV–Vis spectral area [350–420 nm]): (a–c, e, g) $AgNO_3$ concentration (mM) versus reaction time (s); (d, f) plant material quantity (g) versus $AgNO_3$ concentration (mM). Depicts three-dimensional (3D) response surface plots and their corresponding two-dimensional (2D) contour plots.

Şekil 4. İşlem parametrelerinin AgNP verimi üzerindeki etkisi (UV–Vis spektral alanı [350–420 nm] ile belirlenmiştir): $AgNO_3$ konsantrasyonuna (mM) karşı reaksiyon süresi (sn) (a–c, e, g); bitki materyali miktarına karşı $AgNO_3$ konsantrasyonu (mM) (d, f). Üç boyutlu (3D) yanıt yüzeyi grafiklerini ve bunlara karşılık gelen iki boyutlu (2D) kontür grafiklerini göstermektedir.

Validating the Model's Predictive Power

Model validation compared predicted AgNP yields (62.14 for black tea, 48.73 for linden, 58.35 for cherry laurel, 44.23 for kale, and 59.40 for melocan) with experimental yields obtained under optimal condition (9.6 g plant material, 80°C extraction heating temperature, 20 min extraction heating time, 10 mM $AgNO_3$ concentration, 2.5 mL extract volume, 800 W microwave power, and 90 s reaction time). Experimental yields of 63.35, 53.78, 61.95, 45.80, and 61.98, respectively, showed strong agreement with predictions, corresponding to 90.6% to 98.10% validation accuracy. This confirms the model's efficacy in predicting optimal AgNP synthesis conditions and highlights its robustness and potential for practical application in optimizing AgNP synthesis from various plant extracts.

Synthesized-AgNP Characterization

FT–IR spectroscopy

FT–IR analysis of the plant extracts revealed functional groups critical to AgNP synthesis (Figure 5). A broad peak between 3865.30 and 3217.3 cm^{-1} corresponded to O–H stretching vibrations in hydroxyl groups, characteristic of phenolic compounds and aromatic structures (Nikaeen et al., 2020; Jyoti et al., 2016; Türkkan & Gürel, 2024). The sharp peak at 3618.46 cm^{-1} was attributed to C–H stretching in alkanes (not alkynes, which typically appear near 3300 cm^{-1}). Peaks at 2931.8 cm^{-1} (C–H stretching in aliphatic hydrocarbons) and the band spanning 2360.8–1743.7 cm^{-1} (C≡N stretching in nitriles, C≡C in alkynes, and C=O stretching in carbonyl groups) further indicated diverse functional groups. The region 1589.3–1049.3 cm^{-1} encompassed vibrations from C=C aromatic rings, C=O esters, C–O–C ethers, and C–N amines (Shameli et al., 2012; Adnan et al., 2020). Peaks below 887–663.5 cm^{-1} confirmed aromatic C–H bending and phenyl group vibrations. For synthesized AgNPs, FT–IR spectra exhibited a new peak at 2090.8 cm^{-1} (Figure 5), within the range reported for C≡C or metal-ligand interactions (Laime-Oviedo et al., 2023), suggesting involvement in Ag^+ reduction and nanoparticle stabilization. Notably, this peak was absent in black tea-derived AgNPs, likely due to differences in extract composition. Overall, hydroxyl (–OH), amine ($–NH_2$), and carbonyl (–C=O) groups in the plant extracts were pivotal for AgNP formation, acting as both reducing and stabilizing agents.

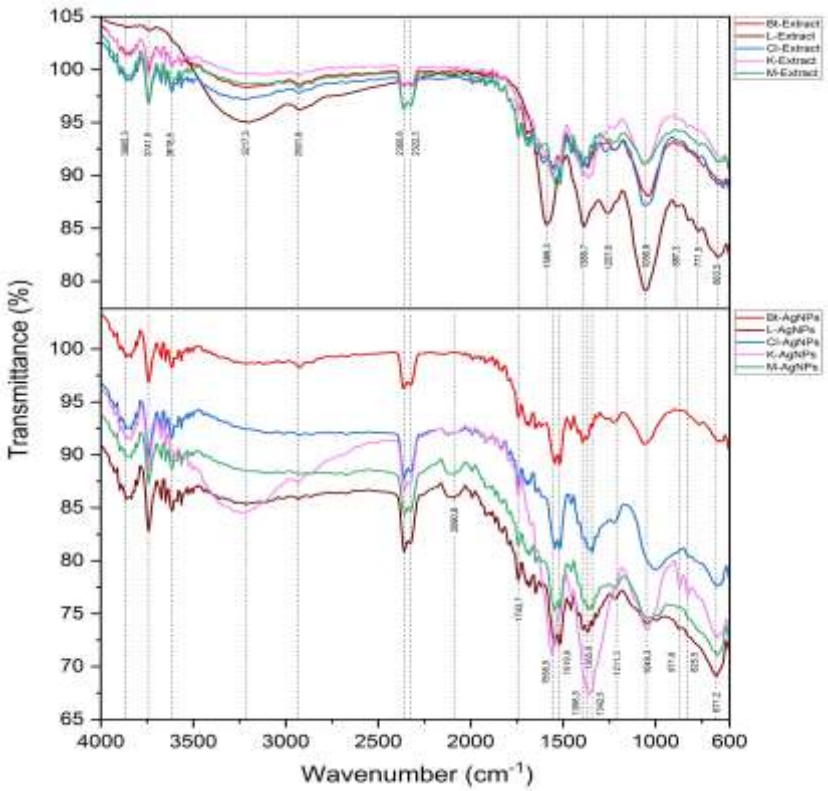

Figure 5. FT–IR spectra of plant extracts (black tea [Bt], linden [L], cherry laurel [Cl], kale [K], and melocan [M]) and their corresponding synthesized silver nanoparticles (Bt-, L-, Cl-, K-, and M-AgNPs).

Şekil 5. Bitki ekstraktlarının (siyah çay [Bt], ıhlamur [L], karayemiş [Cl], yaprak lahana [K] ve melocan [M]) ve bunlara karşılık gelen sentezlenmiş AgNP'lerin (Bt-, L-, Cl-, K- ve M-AgNP'ler) FT–IR spektrumları.

Microscopic and elemental analysis

SEM (Figure 6a–e) and TEM (Figure 6f–j) analyses revealed spherical AgNPs with good dispersion and minimal aggregation. Particle size analysis showed sizes ranging from 3.00 to 25.00 nm, with average sizes of 5.30±0.15 nm for black tea, 8.74±0.42 nm for linden, 7.20±0.17 nm for cherry laurel, 6.32±0.15 nm for kale, and 9.44±0.14 nm for melocan (Figure 6k–o). EDS analysis confirmed the presence of metallic silver (Ag) through a distinct peak at 3 keV (Figure 7a–e), further supported by the observed surface plasmon resonance (SPR) phenomenon, a characteristic signature of metallic AgNPs (Magudapathy et al., 2001; Vijayaraghavan et al., 2012; Karakaş et al., 2024; Türkkan & Gürel, 2024).

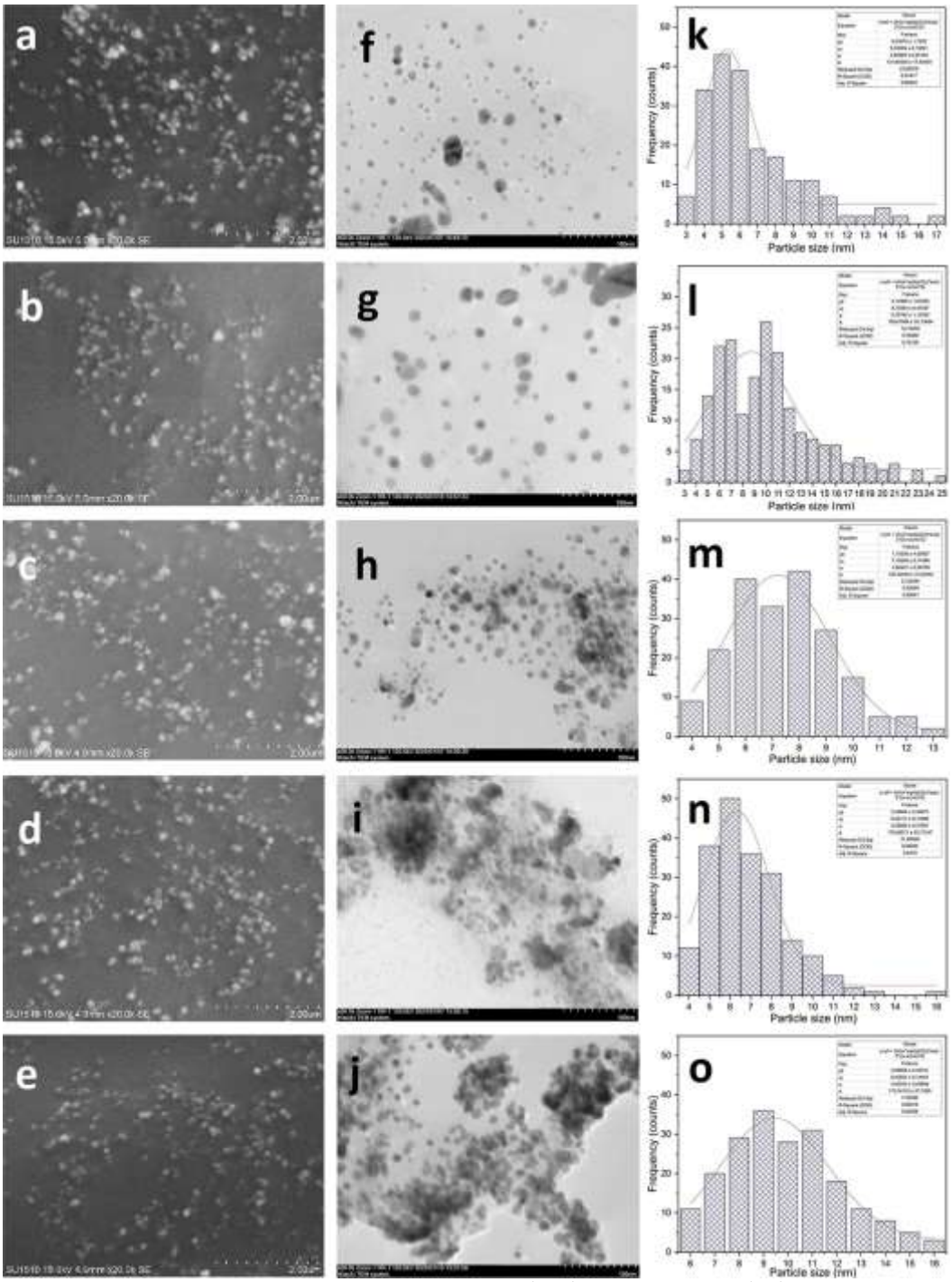

Figure 6. Characterization of Bt-, L-, Cl-, K-, and M-AgNPs. (a–e) SEM images, (f–j) TEM images, and (k–o) size distributions.

Şekil 6. Bt-, L-, Cl-, K- ve M-AgNP'lerin karakterizasyonu. (a–e) SEM görüntüleri, (f–j) TEM görüntüleri, ve (k–o) boyut dağılımları

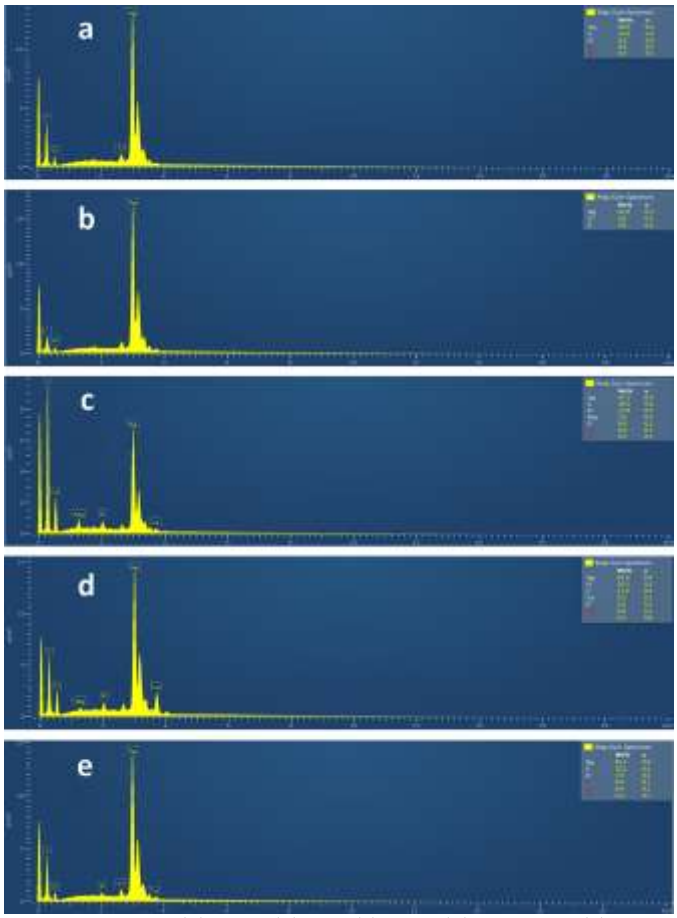

Figure 7. EDS spectra of (a) Bt-, (b) L-, (c) Cl-, (d) K-, and (e) M-AgNPs.
Şekil 7. Bt- (a), L- (b), Cl- (c), K- (d) ve M- (e) AgNP'lerin EDS spektrumları

Antifungal Activity of the Synthesized AgNPs

The antifungal efficacy of AgNPs synthesized from black tea, linden, cherry laurel, kale, and melocan was evaluated against five *Phytophthora* isolates (Table 6). AgNPs derived from different plant sources exhibited variable antifungal effects. Notably, linden- and kale-derived AgNPs showed superior activity, with *P. palmivora* being the most susceptible species. EC_{50} values, reflecting antifungal potency, ranged from 0.76 to 1058.27 µg mL^{-1} across isolates. Linden- and melocan- derived AgNPs did not completely inhibit any isolate at the highest tested concentration (400 µg mL^{-1}), whereas cherry laurel-derived AgNPs achieved complete inhibition of *P. cinnamomi* (Figure 8). Black tea-derived AgNPs at 300 µg mL^{-1} fully inhibited three other *Phytophthora* isolates but failed to suppress *P. cinnamomi* and *P. citrophthora* even at 400 µg mL^{-1}. In contrast, kale-derived AgNPs completely inhibited all five *Phytophthora* isolates at 200 or 300 µg mL^{-1}. Regarding fungicidal activity, cherry laurel-derived AgNPs exhibited fungicidal effects against *P. cinnamomi* at 400 µg mL^{-1}. Black tea-derived AgNPs were fungicidal for *P. capsici* and *P. nicotianae* at 300 µg mL^{-1} and for *P. palmivora* at 400 µg mL^{-1}. Kale-derived AgNPs showed fungicidal activity against *P. capsici* at 200 µg mL^{-1} and against the remaining four *Phytophthora* isolates at 400 µg mL^{-1}. These findings align with prior reports on AgNP minimum fungicidal concentrations (MFCs). For instance, Yiğit et al. (2023) documented cherry laurel-AgNP MFCs exceeding 150 µg mL^{-1} against oomycete and fungal pathogens, while Yiğit & Türkkan (2023) observed linden-AgNP MFCs ranging from 225 to 900 µg mL^{-1} for *Phytophthora* species. Türkkan & Gürel (2024) reported Madimak-AgNP MFCs of 400–800 µg mL^{-1} against related species (*P. cactorum, P. capsici, P. cinnamomi, P. citrophthora, P. nicotianae, P. megaspermae/P. palmivora*). In contrast, wormwood-derived AgNPs demonstrated stronger antifungal activity against *Phytophthora* species, with MICs well below 100 µg mL^{-1} (Ali et al., 2007), emphasizing the critical role of plant source in shaping AgNP efficacy. The observed variability in antifungal performance underscores the intricate relationship between AgNP properties (e.g., size, shape, surface chemistry) and their biological targets. Further research is required to unravel how plant-specific phytochemicals modulate AgNP characteristics and interactions with pathogens. These variations highlight the importance of nanoparticle design in optimizing antimicrobial applications. Upon entering microbial cells, AgNPs disrupt essential cellular functions, ultimately leading to cell death (Buzea, 2007).

Table 6. *In vitro* antifungal activity of synthesized AgNPs against *Phytophthora* species
Çizelge 6. Sentezlenmiş AgNP'lerin Phytophthora türlerine karşi in vitro antifungal aktivitesi

Plant-AgNPs	*Phytophthora* spp.	Mycelial growth (cm) (400 µg mL^{-1})			EC_{50}[b] (µg mL^{-1})	MIC[c] (µg mL^{-1})	MFC[d] (µg mL^{-1})
Black tea-AgNPs	*P. capsici*	0.00	±	0.00[a]	40.88	300	300
	P. cinnomami	1.61	±	0.12	36.67	>400	>400
	P. citrophthora	4.08	±	0.17	168.66	>400	>400
	P. nicotianae	0.00	±	0.00	45.73	300	300
	P. palmivora	0.00	±	0.00	48.53	300	400
Linden-AgNPs	*P. capsici*	0.95	±	0.12	3.69	>400	>400
	P. cinnomami	1.68	±	0.08	0.80	>400	>400
	P. citrophthora	1.72	±	0.02	9.60	>400	>400
	P. nicotianae	1.93	±	0.04	4.45	>400	>400
	P. palmivora	1.16	±	0.04	0.76	>400	>400
Chery laurel-AgNPs	*P. capsici*	1.20	±	0.05	58.52	>400	>400
	P. cinnomami	0.00	±	0.00	57.36	400	400
	P. citrophthora	4.77	±	0.08	225.37	>400	>400
	P. nicotianae	2.32	±	0.07	62.84	>400	>400
	P. palmivora	2.80	±	0.26	99.48	>400	>400
Kale-AgNPs	*P. capsici*	0.00	±	0.00	21.10	200	200
	P. cinnomami	0.00	±	0.00	21.62	300	400
	P. citrophthora	0.00	±	0.00	18.13	300	400
	P. nicotianae	0.00	±	0.00	30.84	300	400
	P. palmivora	0.00	±	0.00	9.28	300	400
Melocan-AgNPs	*P. capsici*	6.00	±	0.35	284.48	>400	>400
	P. cinnomami	7.88	±	0.20	199.14	>400	>400
	P. citrophthora	17.10	±	0.28	>400	>400	>400
	P. nicotianae	7.25	±	0.18	210.91	>400	>400
	P. palmivora	5.79	±	0.33	201.67	>400	>400

[a]Data are presented as means ± standard errors. [b]The concentration that caused 50% reduction, [c]Minimum inhibitory concentration, [d]Minimum fungicidal concentration.

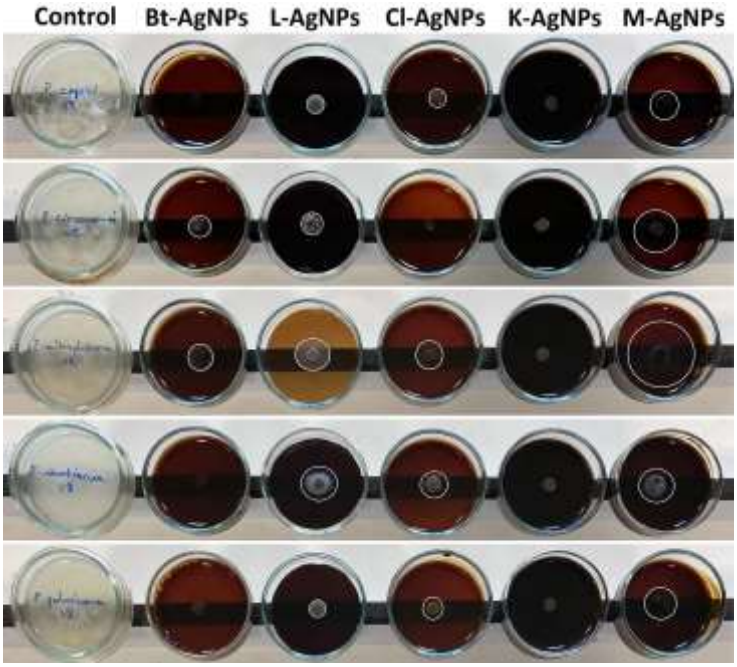

Figure 8. Inhibitory effects of AgNPs synthesized from black tea (Bt), linden (L), cherry laurel (Cl), kale (K), and melocan (M) on *Phytophthora* species at a concentration of 400 µg mL^{-1}.
Şekil 8. Siyah çay (Bt), ıhlamur (L), karayemiş (Cl), yaprak lahana (K) ve melocan (M)'dan sentezlenmiş AgNP'lerin 400 µg mL^{-1} konsantrasyonda Phytophthora türleri üzerindeki engelleyici etkisi.

CONCLUSION

This study successfully demonstrated the green synthesis of silver nanoparticles (AgNPs) using aqueous extracts of black tea, linden, cherry laurel, kale, and melocan. UHPLC and UV–Vis analyses identified a diverse array of bioactive compounds, including phenolic acids (e.g., gallic acid) and putative flavonoids, which likely facilitated the reduction of Ag^+ ions and stabilization of the nanoparticles. Through statistical optimization via Plackett–Burman and Box–Behnken designs, the following optimal synthesis conditions were established: 9.6 g of plant material, extraction heating at 80°C for 20 minutes, 10 mM $AgNO_3$, 2.5 mL extract volume, 800 W microwave power, and a 90-second reaction time. Characterization revealed uniform, spherical AgNPs with sizes ranging from 3.00 to 25.00 nm (determined by TEM), with plant-specific averages of 5.30 nm (black tea), 8.74 nm (linden), 7.20 nm (cherry laurel), 6.32 nm (kale), and 9.44 nm (melocan). The synthesized AgNPs exhibited significant antifungal activity against key *Phytophthora* pathogens (*P. capsici, P. cinnamomi, P. citrophthora, P. nicotianae*, and *P. palmivora*), with kale-derived AgNPs showing exceptional dual fungistatic and fungicidal effects. These findings highlight the potential of plant-mediated AgNPs as a sustainable alternative for managing fungal diseases in agriculture. Future research should focus on field trials to assess practical efficacy, mechanistic studies to elucidate nanoparticle-pathogen interactions, and scalability assessments for large-scale agricultural applications.

ACKNOWLEDGMENTS

This research was supported by the Ordu University Scientific Research Projects Unit (BAP), project number B-2209. The authors thank Dr. İlker Kurbetli for the *Phytophthora* isolates, Dr. Umut Ateş for the HPLC analyses, and Dr. Hamdi Güray Kutbay for the melocan (*Smilax excelsa* L.) botanical identification.

Contribution of the Authors as Summary

The authors declare that they have contributed equally to the article.

Conflict of Interest

The authors declare no conflicts of interest.

REFERENCES

Adnan, M., Azad, M. O. K., Madhusudhan, A., Saravanakumar, K., Hu, X., Wang, M. H. & Ha, C. D. (2020). Simple and cleaner system of silver nanoparticle synthesis using kenaf seed and revealing its anticancer and antimicrobial potential. *Nanotechnology, 31*(26), 265101. https://doi.org/10.1088/1361-6528/ab7d72

Ahmad, N. & Sharma, S. (2012). Green Synthesis of silver nanoparticles using extracts of *Ananas comosus*. *Green and Sustainable Chemistry, 2*(4), 1-7. https://doi.org/10.4236/gsc.2012.24020

Akyuz, E., Şahin, H., Islamoglu, F., Kolayli, S. & Sandra, P. (2014). Evaluation of phenolic compounds in *Tilia rubra* subsp. *caucasica* by HPLC–UV and HPLC–UV–MS/MS. *International Journal of Food Properties, 17*, 331-343. https://doi.org/10.1080/10942912.2011.631252

Ali, M., Kim, B., Belfield, K. D., Norman, D., Brennan, M. & Ali, G. S. (2015). Inhibition of *Phytophthora parasitica* and *P. capsici* by silver nanoparticles synthesized using aqueous extract of *Artemisia absinthium*. *Phytopathology, 105*(9), 1183-1190. https://doi.org/10.1094/PHYTO-01-15-0006-R

Baytop, T. (1999). Therapy with medicinal plants in Turkey (past and present). Publication of the Istanbul University, 312.

Box, G. E. P. & Behnken, D. W. (1960). Simplex-sum designs: a class of second order rotatable designs derivable from those of first order. *The Annals of Mathematical Statistics, 31*(4), 838-864. https://doi.org/10.1214/aoms/1177705661

Buzea, C., Pacheco, I. I. & Robbie, K. (2007). Nanomaterials and nanoparticles: sources and toxicity. *Biointerphases 2*(4), MR17-MR71. https://doi.org/10.1116/1.2815690

Cai, Y., Piao, X., Gao, W., Zhang, Z., Nie, E. & Sun, Z. (2017). Large-scale and facile synthesis of silver nanoparticles via a microwave method for a conductive pen. *RSC Advances, 7*(54), 34041-34048. https://doi.org/10.1039/C7RA05125E

Chowdhury, S., Yusof, F., Faruck, M. O. & Sulaiman, N. (2016). Process optimization of silver nanoparticle synthesis using response surface methodology. *Procedia Engineering, 148*, 992-999. https://doi.org/10.1016/j.proeng.2016.06.552

Davis, P., Tan, K. & Mill, R.R. (1988). Flora of Turkey and the East Aegean Islands and Supplement I. Edinburgh University Press, Edinburgh.

El-Sawaf, A. K., El-Moslamy, S. H., Kamoun, E. A., & Hossain, K. (2024). Green synthesis of trimetallic CuO/Ag/ZnO nanocomposite using *Ziziphus spina-christi* plant extract: characterization, statistically

experimental designs, and antimicrobial assessment. *Scientific Reports, 14*(1), 19718. https://doi.org/10.1038/s41598-024-67579-5

Encu, S. (2010). *Lahana çeşitlerinin antioksidan kapasiteleri ve bileşenleri açısından değerlendirilmesi (Tez no 282642)*. [Yüksek Lisans Tezi, İstanbul Üniversitesi Fen Bilimleri Enstitüsü Kimya Ana Bilim Dalı]. Yükseköğretim Kurulu Ulusal Tez Merkezi.

Günal, N. (2013). Türkiye'de iklimin doğal bitki örtüsü üzerindeki etkileri. *Acta Turcıca Çevrimiçi Tematik Türkoloji Dergisi,* V(1), 1-22.

Fazil, M. M., Gul, A. & Jawed, H. (2024). Optimization of silver nanoparticles synthesis via Plackett–Burman experimental design: *in vitro* assessment of their efficacy against oxidative stress-induced disorders. *RSC Advances*, *14*(29), 20809-20823. https://doi.org/10.1039/d4ra02774d

Firoozi, S., Jamzad, M. & Yari, M. (2016). Biologically synthesized silver nanoparticles by aqueous extract of *Satureja intermedia* C.A. Mey and the evaluation of total phenolic and flavonoid contents and antioxidant activity. *Journal of Nanostructure in Chemistry, 6*, 357-364. https://doi.org/10.1007/s40097-016-0207-0

Gevrek, C., Yiğit, U. & Türkkan, M. (2023). Optimization and antifungal activity of silver nanoparticles synthesized using the leaf extract of *Corylus colurna* L. (Turkish hazelnut). *Akademik Ziraat Dergisi, 12*(Özel Sayı), 159-172. https://doi.org/10.29278/azd.1335259

Halima, R., Narula, A. & Sravanthi, V. (2021). Optimization of process parameters for the green synthesis of silver nanoparticles using Plackett–Burman and 3-level Box–Behnken Design. *Journal of Huazhong University of Science and Technology, 50*(3), 1-17.

İslam, A. & Deligöz, H. (2012). Ordu ilinde karayemiş (*Laurocerasus officinalis* L.) seleksiyonu. *Akademik Ziraat Dergisi, 1*(1), 37-44.

Jyoti, K., Baunthiyal, M. & Singh, A. (2016). Characterization of silver nanoparticles synthesized using *Urtica dioica* Linn. leaves and their synergistic effects with antibiotics. *Journal of Radiation Research and Applied Sciences, 9*(3), 217-227. https://doi.org/10.1016/j.jrras.2015.10.002

Kale, R., Barwar, S., Kane, P. & More, S. (2018). Green synthesis of silver nanoparticles using papaya seed and its characterization. *International Journal for Research in Applied Science & Engineering Technology, 6*, 168-174. https://doi.org/10.22214/ijraset.2018.2026

Karabegović, I.T., Stojicevi´c, S.S., Velickovic, D.T., Zoran B. Todorovic, Z.B., Nada C. Nikolic, N.C., Miodrag L. & Lazic, M.L. (2014). The effect of different extraction techniques on the compositionand antioxidant activity of cherry laurel (*Prunus laurocerasus*) leaf and fruit extracts. *Industrial Crops and Products, 54*, 142-148. https://doi.org/10.1016/j.indcrop.2013.12.047

Karakaş, İ., Hacıoğlu, N. & Özdemir, B. E. (2024). Green synthesis and antibiofilm activity of silver nanoparticles by *Camellia sinensis* L. (White tea leaf). *Kahramanmaraş Sütçü İmam Üniversitesi Tarım ve Doğa Dergisi, 27*(2), 285-292. https://doi.org/10.18016/ksutarimdoga.1297130

Kelly, K. L., Coronado, E., Zhao, L. L. & Schatz, G. C. (2003). The optical properties of metal nanoparticles: the influence of size, shape, and dielectric environment. *The Journal of Physical Chemistry B, 107*(3), 668-677. https://doi.org/10.1021/jp026731y

Kolaylı, S., Kucuk, M., Duran, C., Candan, F. & Dinçer, B. (2003). Chemical and antioxidant properties of *Laurocerasus officinalis* Roem. (Cherry laurel) fruit grown in the Black Sea Region. *Journal of Agricultural and Food Chemistry, 51*, 7489-94. https://doi.org/10.1021/jf0344486

Konwarh, R., Karak, N., Sawian, C. E., Baruah, S. & Mandal, M. (2011). Effect of sonication and aging on the templating attribute of starch for "green" silver nanoparticles and their interactions at biointerface. *Carbohydrate Polymers, 83*(3), 1245-1252. https://doi.org/10.1016/j.carbpol.2010.09.031

Kumar, K. M., Sinha, M., Mandal, B. K., Ghosh, A. R., Kumar, K. S. & Reddy, P. S. (2012). Green synthesis of silver nanoparticles using *Terminalia chebula* extract at room temperature and their antimicrobial studies. *Spectrochimica Acta Part A: Molecular and Biomolecular Spectroscopy, 91*, 228-233. https://doi.org/10.1016/j.saa.2012.02.001

Laime-Oviedo, L. A., Soncco-Ccahui, A. A., Peralta-Alarcon, G., Arenas-Chávez, C. A., Pineda-Tapia, J. L., Díaz-Rosado, J. C. & Vera-Gonzales, C. (2022). Optimization of synthesis of silver nanoparticles conjugated with *Lepechinia meyenii* (Salvia) using Plackett–Burman Design and Response Surface Methodology—preliminary antibacterial activity. *Processes, 10*(9), 1727. https://doi.org/10.3390/pr10091727

Laime-Oviedo, L. A., Arenas-Chávez, C. A., Yáñez, J. A. & Vera-Gonzáles, C. A. (2023). Plackett–Burman design in the biosynthesis of silver nanoparticles with *Mutisia acuminatta* (Chinchircoma) and preliminary evaluation of its antibacterial activity. *F1000Research*, 12. https://doi.org/10.12688/f1000research.140883.1

Magudapathy, P., Gangopadhyay, P., Panigrahi, B. K., Nair, K. G. M. & Dhara, S. (2001). Electrical transport studies of Ag nanoclusters embedded in glass matrix. *Physica B: Condensed Matter, 299*(1-2), 142-146. https://doi.org/10.1016/S0921-4526(00)00580-9

Naveed M., BiBi J., Kamboh A. A., Suheryani I., Kakar, I., Fazlani, S. A., FangFang, X., Kalhoro, S. A., Yunjuan L, Kakar, M. U, Abd El-Hack, M. E., Noreldin, A. E., Zhixiang, S., LiXia, C. & XiaoHui, Z. (2018). Pharmacological values and therapeutic properties of black tea (*Camellia sinensis*): A comprehensive overview. *Biomed Pharmacotherapy, 100*, 521-531. https://doi.org/10.1016/j.biopha.2018.02.048

Nikaeen, G., Yousefinejad, S., Rahmdel, S., Samari, F. & Mahdavinia, S. (2020). Central composite design for optimizing the biosynthesis of silver nanoparticles using *Plantago major* extract and investigating antibacterial, antifungal and antioxidant activity. *Scientific Reports, 10*(1), 9642. https://doi.org/10.1038/s41598-020-66357-3

Noroozi, M., Zakaria, A., Moksin, M. M., Wahab, Z. A. & Abedini, A. (2012). Green formation of spherical and dendritic silver nanostructures under microwave irradiation without reducing agent. *International Journal of Molecular Sciences, 13*(7), 8086-8096. https://doi.org/10.3390/ijms13078086

Othman, L., Sleiman, A., & Abdel-Massih, R. M. (2019). Antimicrobial activity of polyphenols and alkaloids in Middle eastern plants. *Frontiers in Microbiology*,*10*, 911. https://doi.org/10.3389/fmicb.2019.00911.

Ovais, M., Khalil, A. T., Islam, N. U., Ahmad, I., Ayaz, M., Saravanan, M. & Mukherjee, S. (2018). Role of plant phytochemicals and microbial enzymes in biosynthesis of metallic nanoparticles. *Applied Microbiology and Biotechnology, 102*, 6799-6814. https://doi.org/10.1007/s00253-018-9146-7

Öz, M. (2022). *Tilia rubra* DC. subsp. *caucasica* V.Engler (Kafkas Ihlamuru) yaprak uçucu yağının kimyasal bileşimi. III. International Siirt Scientific Research Congress, Siirt, Türkiye, 18-19 November 2022, ss.14.

Özsoy, N., Can, A., Yanardag, R. & Akev, N. (2008). Antioxidant activity of *Smilax excelsa* L. leaf extracts. *Food Chemistry, 110*(3), 571-583. https://doi.org/10.1016/j.foodchem.2008.02.037

Özturk, B., Yıldız, K. & Küçüker, E. (2015). Effect of pre-harvest methyl jasmonate treatments on ethylene production, water-soluble phenolic compounds and fruit quality of Japanese plums. *Journal of the Science of Food and Agriculture, 95*(3), 583-591. https://doi.org/10.1002/jsfa.6787

Plackett, R. L. & Burman, J. P. (1946). The design of optimum multifactorial experiments. *Biometrika, 33*(4), 305-325. https://doi.org/10.1093/biomet/33.4.305

Reddy, L. V. A., Wee, Y. J., Yun, J. S. & Ryu, H. W. (2008). Optimization of alkaline protease production by batch culture of *Bacillus* sp. RKY3 through Plackett–Burman and response surface methodological approaches. *Bioresource Technology, 99* (7), 2242-2249. https://doi.org/10.1016/j.biortech.2007.05.006

Sahan, Y. (2011). Effect of *Prunus laurocerasus* L. (Cherry laurel) leaf extracts on growth of bread spoilage fungi. *Bulgarian Journal of Agricultural Science, 17* (1), 83-92.

Šamec, D., Urlić, B. & Salopek-Sondi, B. (2018). Kale (*Brassica oleracea* var. *acephala*) as a superfood: Review of the scientific evidence behind the statement. *Critical Reviews in Food Science and Nutrition, 59*(15), 2411-2422. https://doi.org/10.1080/10408398.2018.1454400

Shah, M., Fawcett, D., Sharma, S., Tripathy, S. K. & Poinern, G. E. J. (2015). Green synthesis of metallic nanoparticles via biological entities. *Materials, 8*(11), 7278-7308. https://doi.org/10.3390/ma8115377

Shameli, K., Bin Ahmad, M., Jaffar Al-Mulla, E. A., Ibrahim, N. A., Shabanzadeh, P., Rustaiyan, A. & Zidan, M. (2012). Green biosynthesis of silver nanoparticles using *Callicarpa maingayi* stem bark extraction. *Molecules, 17*(7), 8506-8517. https://doi.org/10.3390/molecules17078506

Sharma, N. K., Vishwakarma, J., Rai, S., Alomar, T. S., AlMasoud, N. & Bhattarai, A. (2022). Green route synthesis and characterization techniques of silver nanoparticles and their biological adeptness. *ACS Omega, 7*(31), 27004-27020. https://doi.org/10.1021/acsomega.2c01400

Siddiqi, K.S., Husen, A. & Rao, R.A.K. (2018). A review on biosynthesis of silver nanoparticles and their biocidal properties. *Journal of Nanobiotechnology, 16,* 14. https://doi.org/10.1186/s12951-018-0334-5

Siddiqui, A., Gul, A., Khan, H., Anjum, F. & Hussain, T. (2024). Bio-inspired synthesis of silver nanoparticles using *Salsola imbricata* and its application as antibacterial additive in glass ionomer cement. *Nanotechnology, 35*(35), 355101. https://doi.org/10.1088/1361-6528/ad50e4

Singleton, V. L. & Rossi, J. A. (1965). Colorimetry of total phenolics with phosphomolybdic-phosphotungstic acid reagents. *American Journal of Enology and Viticulture, 16*(3), 144-158. https://doi.org/10.5344/ajev.1965.16.3.144

Singleton, V.L. (1999). Analysis of total phenols and other oxidation substrates and antioxidants by means of Folin-Ciocalteu reagent. *Methods in Enzymology, 299*, 152-178.

Stepanov, A. L. (2004). Optical properties of metal nanoparticles synthesized in a polymer by ion implantation: a review. *Technical Physics, 49,* 143-153. https://doi.org/10.1134/1.1648948

Trivedi, P., Khandelwal, M. & Srivastava, P. (2014). Statistically optimized synthesis of silver nanocubes from peel extracts of *Citrus limetta* and potential application in waste water treatment. *Journal of Microbial & Biochemical Technology, 4*(004). https://doi.org/10.4172/1948-5948.S4-004

Tuttu, G., Ursavaş, S. & Söyler, R. (2017). Ihlamur çiçeğinin Türkiye'deki hasat miktarları ve etnobotanik kullanımı. *Anadolu Orman Araştırmaları Dergisi, 3*(1), 60-66

Türkkan, M. & Gürel, Y. (2024). Plackett–Burman and Box–Behnken Designs for optimizing *Polygonum cognatum* Meissn-mediated AgNP synthesis: Antifungal activity against diverse *Phytophthora* spp. *Akademik Ziraat Dergisi, 13*(2), 272-286. https://doi.org/10.29278/azd.1522321

Vijayaraghavan, K., Nalini, S. K., Prakash, N. U. & Madhankumar, D. J. M. L. (2012). Biomimetic synthesis of silver nanoparticles by aqueous extract of *Syzygium aromaticum*. *Materials Letters, 75,* 33-35. https://doi.org/10.1016/j.matlet.2012.01.083

Ye, M., Yang, W., Zhang, M., Huang, H., Huang, A. & Qiu, B. (2023). Biosynthesis, characterization, and antifungal activity of plant-mediated silver nanoparticles using *Cnidium monnieri* fruit extract. *Frontiers in Microbiology, 14,* 1291030. https://doi.org/10.3389/fmicb.2023.1291030

Yeşilada, E., Sezik, E., Honda, G., Takasihi, Y., Takeda, Y. & Tanaka, T. (1999). Traditional medicine in Turkey IX. Folk Medicine in Noth-West Anatolia. *Journal of Ethnopharmacology, 64*, 195- 210

Yiğit, U. & Türkkan, M. (2023). Antifungal activity and optimization procedure of microwave-synthesized silver nanoparticles using linden (*Tilia rubra* subsp. *caucasica*) flower extract. *International Journal of Chemistry and Technology, 7*(1), 25-37. https://doi.org/10.32571/ijct.1194356

Yiğit, U., Gürel, Y., Ilhan, H. & Türkkan, M. (2023). Antifungal activity and optimization procedure of silver nanoparticles green synthesized with *Prunus laurocerasus* L. (Cherry laurel) leaf extract. *International Journal of Life Sciences and Biotechnology, 6* (1), 1–20. https://doi.org/10.38001/ijlsb.1168628

Yilmaz, M., Yilmaz, A., Karaman, A., Aysin, F. & Aksakal, O. (2021). Monitoring chemically and green-synthesized silver nanoparticles in maize seedlings via surface-enhanced Raman spectroscopy (SERS) and their phytotoxicity evaluation. *Talanta, 225*, 121952. https://doi.org/10.1016/j.talanta.2020.121952